
Unlocking Text Capabilities in Vision Models

Fawaz Sammani^{1,2,3}, Jonas Fischer¹, Nikos Deligiannis^{2,3}

¹Max-Planck-Institut für Informatik, Saarbrücken, Germany

²ETRO Department, Vrije Universiteit Brussel, Belgium

³imec, Leuven, Belgium

`fawaz.sammani@vub.be`, `jonas.fischer@mpi-inf.mpg.de`, `ndeliglia@etrovub.be`

Abstract

Visual classifiers provide high-dimensional feature representations that are challenging to interpret and analyze. Text, in contrast, provides a more expressive and human-friendly interpretable medium for understanding and analyzing model behavior. We propose a simple, yet powerful method for reformulating any pretrained visual classifier so that it can be queried with free-form text without compromising its original performance. Our approach is label-free, data and compute-efficient, and is trained to preserve the underlying classifier’s distribution and decision-making processes. Our method unlocks several zero-shot text interpretability applications for any visual classifier. We apply our method on 40 visual classifiers and demonstrate two primary applications: 1) building both label-free and zero-shot concept bottleneck models and therefore converting *any* visual classifier to be inherently-interpretable and 2) zero-shot decoding of visual features into natural language sentences. In both tasks we establish new state-of-the-art results, outperforming existing works and surpassing CLIP-based baselines with ImageNet-only trained classifiers, while using up to $400\times$ fewer images and $400,000\times$ less text during training.

1 Introduction

Visual classifiers provide dense, high-dimensional visual feature vectors that are difficult to interpret directly. Attribution maps—the standard way to interpret visual classifiers—only highlight the image region most influential to a prediction, offering a high-level spatial insight. They reveal where the key features lie, but not what those features actually mean or represent. By contrast, text is significantly more expressive, more precise and human-friendly, and it enables a new suite of text interpretability tasks [1, 2, 3]. This raises a key question: *How can we query a purely visual classifier with free-form text?* Performing this allows us to have a text interface that can be used to query visual classifiers. Contrastive Language-Image Pre-Training (CLIP)-based vision–language models answer this by learning a shared embedding space [4], enabling any text to query the visual model directly. Yet in many real-world scenarios a high-performing, task-specific *legacy* model already exists and typically outperforms zero-shot vision–language models [5]. Retraining such a specialist on a large image–text corpus following the CLIP approach or the GPT-like approach is impractical, in terms of computational cost and need of a huge amount of image–text data. Moreover, this approach alters the decision-making process and distribution of the legacy model. As a result, most text-based interpretability techniques remain confined to CLIP-like models, leaving specialist vision models without a language-driven interface.

In this work, we lift this limitation by proposing a method to reformulate any frozen visual classifier such that it can be accessed via free-form text (Figure 1). Our method is characterized by four important properties: First, it is *efficient*; it is inexpensive to train and can be performed on any standard hardware, regardless of the size of the original classifier. The number of data points is



Figure 1: **(a)** Text interpretability is typically limited to models trained to share a joint embedding space such as CLIP-based ones. **(b)** Our approach removes this constraint, enabling any visual classifier to be queried through any arbitrary (unaligned) text encoder in a highly data- and compute-efficient, label-free manner, while preserving the classifier’s original distribution and reasoning process and thus offering text-based interpretability of the original classifier. The values here represent the cosine similarity between the text and the visual features f .

also significantly reduced compared to CLIP-based approaches. Secondly, it is *label-free*, no labels are required to achieve this formulation. Thirdly, it is explicitly *trained to preserve* the original distribution and reasoning process of the classifier. Finally, our method is applicable to *any* vision architecture, whether convolutional-based, transformer-based or hybrid.

A visual classifier assigns an image to a specific category from a predefined set of discrete class labels. In ImageNet-1K [6], this set contains 1,000 class labels. Originally, these discrete class labels correspond to class names in text format. For example, in ImageNet-trained models, the discrete label 1 corresponds to the class *goldfish*. These classes are typically discretized to facilitate training with cross-entropy. However, when the textual class names are embedded into vector representations (*e.g.*, using a text encoder or word embedding model), they provide semantic information. Specifically, these embeddings reside in a continuous space where nearby vectors capture related concepts. For the “goldfish” example, neighboring vectors might include “freshwater”, “fins” and “orange”. Our method learns to map images into this text embedding space using *only* class names, thus associating both the class name *and its surrounding semantic space* with the image. This is accomplished through a trainable multilayer perceptron (MLP) that projects the visual features into the text embedding space, and is explicitly trained to output the same distribution scores across all classes, as the original classifier’s class distribution. This is done while keeping both the visual and textual encoders frozen. By using solely the class names without any supplementary information, we can learn a semantically meaningful image-text space. This allows us to query the visual classifier with any text query beyond the class names.

We demonstrate the effectiveness of our method with two primary applications. 1) We build label-free concept bottleneck models for any pretrained classifier (not being restricted to CLIP) while obtaining the linear probe classifier in a zero-shot manner (we do not train a linear probe on the concept activations), also ensuring that the newly built linear classifier shares the same reasoning process with the original classifier. 2) We show that our method can decode visual features of any classifier into natural language in a zero-shot manner, without requiring training on image-text data such as image-caption pairs, while also showing the generalization of our method to datasets beyond ImageNet.

In summary, our contributions are as follows: **(i)** We propose an efficient, label-free method to reformulate any visual classifier such that it can be queried with open-set text queries, maintaining its performance within a negligible margin (average of 0.2 points drop in accuracy) **(ii)** We demonstrate the effectiveness of our method with 40 different architectures through two applications: label-free zero-shot Concept Bottleneck Models (CBMs) for any visual classifier, and zero-shot decoding of visual features into natural language. **(iii)** On both these applications, our method sets new state-of-the-art results outperforming existing works, including those using CLIP as the visual encoder, while being trained with $400\times$ less images and $400,000\times$ less text data.

2 Related Work

While CLIP is the predominant approach to interpret vision models through language [2], there exist works that try to decode visual features of models beyond CLIP. DeViL [7] and LIMBER [8] trains an autoregressive text generator to map visual features into image captions, leveraging annotated image-caption pairs as ground-truth data. Similarly, Natural Language Explanations (NLEs) [9, 10, 11] use

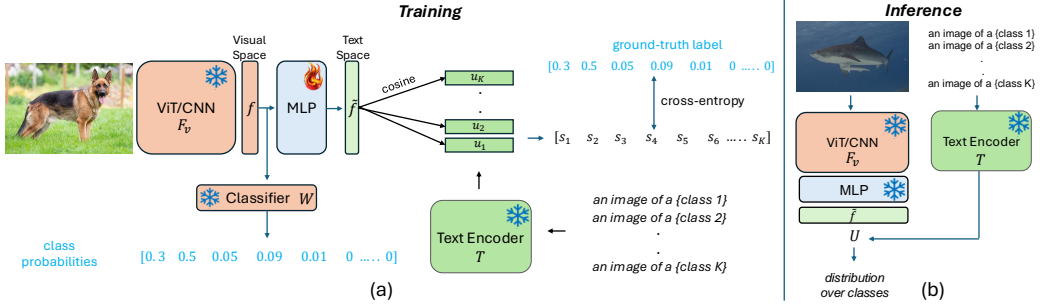


Figure 2: An overview of our method for reformulating visual classifiers. **(a)** The process of training the MLP mapping between vision and text space. A PyTorch-like pseudocode for (a) is included in Section B of the Appendix. **(b)** The process of inference with the adapted visual classifier. The text encoder acts as a linear classifier weight generator in our re-formulated classification process. \circ indicates that the module is frozen, while \heartsuit indicates trainable.

annotated textual explanations in place of conventional captions. Notably, all these works (1) rely on annotated datasets and (2) explicitly train the generated text to align with what annotators want the visual features to describe, thereby altering the classifier’s original reasoning process. ZS-A2T [12] converts attention maps into natural language in a zero-shot manner using LLMs, but is constrained to vision-language models trained to learn a shared vision-language embedding space (e.g., through a contrastive objective); therefore, it cannot be applied to standalone visual classifiers. In contrast, our method decodes visual features of any pretrained classifier in a zero-shot manner without requiring any annotated data, and is explicitly trained to keep the model’s predictive distribution intact.

Text-to-Concept (T2C) [13] and [14] are the closest related works to ours. These works train a linear layer to map image features of any classifier into the CLIP vision encoder space, such that they can be interpreted via text using the CLIP text encoder. Since the linear layer maps features to the CLIP space, these works are strongly biased towards interpreting the CLIP model rather than the original classifier. As the ground-truth data for training the linear mapper are the features extracted from the CLIP vision encoder, this method is approximate to using the CLIP vision encoder directly to encode the image. Moreover, these works rely on CLIP supervision during training. In contrast, our approach is label-free and our mapping function is explicitly trained to preserve the classifier’s original distribution.

3 Method

Consider an image I and a visual classifier F composed of a visual feature extractor F_v and a linear classifier W . Note that F can be of any architecture. F_v embeds I into an n -dimensional feature vector $f \in \mathbb{R}^n$. That is, $f = F_v(I)$. The linear classifier $W \in \mathbb{R}^{n \times K}$ takes f as input and outputs a probability distribution o for the image across K classes. That is, $o = \text{softmax}(f.W) \in \mathbb{R}^K$. For ImageNet-1K, $K = 1000$. Consider also any off-the-shelf text encoder T which takes in an input text l and embeds it into a m -dimensional vector representation $u \in \mathbb{R}^m$. That is, $u = T(l)$. Note that u and f are not in the same space and can have a different number of dimensions, so we cannot query f with the text l .

We propose to learn a simple lightweight MLP mapping function that projects the visual features f into the text embedding space of T , resulting in a new vector \tilde{f} . That is, $\tilde{f} = \text{MLP}(f)$, where $\tilde{f} \in \mathbb{R}^m$. Note that the visual encoder F_v , the linear classifier W , and the text encoder T are all frozen; only the MLP is trainable, making our method *efficient*. We then take the textual class names of the K classes, and convert each into a text prompt l_i^p , represented as: “an image of a {class}” where {class} represents the class name in text format. This results in K textual prompts, each of which is encoded with T : $u_i = T(l_i^p)$, $\forall i = 1, \dots, K$. Stacking all the encoded prompts, we get a matrix $U \in \mathbb{R}^{K \times m}$. Here, U acts as weights of the classification layer for our approach. We then calculate the cosine similarity¹ between each u_i and the visual features f : $s_i = \tilde{f} \cdot u_i$. Equivalently, this can be performed as a single vector-matrix multiplication: $S = \tilde{f} \cdot U^T$, where $S \in \mathbb{R}^K$ represents

¹in the rest of this paper, we will omit the unit norm in cosine similarity to reduce clutter, and represent it with the dot product

the cosine similarity scores between the visual features and every text prompt l_i^p representing a class. In other words, S represents the classification logits of our approach.

The most straightforward way to training the MLP mapper is to leverage the ground-truth labels from the dataset, aligning S with the ground-truth distribution. However, this approach violates two key properties: (1) it necessitates annotated data, and (2) re-training the classifier alters its original distribution o , thereby changing the reasoning process of the classifier (i.e., how it maps visual features to class probabilities and makes predictions) and sacrificing text interpretability of the original classifier. Notably, the original soft probability distribution o is a function of the linear classifier W , so W cannot be ignored. We instead propose to align S to the original distribution o through the cross-entropy loss. For a single sample, the loss is given by:

$$L = - \sum_{i=1}^K o_i \log \left(\frac{e^{s_i}}{\sum_{j=1}^K e^{s_j}} \right). \quad (1)$$

This task can be viewed as a knowledge distillation problem, except that we do not distill the knowledge of a bigger teacher model to a smaller student model, but distill the distribution of the original model to a reformulated way of classification. Note that the loss is equivalent to the KL divergence loss between o and the predicted distribution, since the additional entropy term $H(o)$ that appears in the KL divergence loss is a constant that does not depend on the MLP parameters. Eq. 1 shows that our approach is label-free and steers the MLP to be faithful to the original classifier F , since it is explicitly trained for that purpose. Note also that this loss function naturally encodes the classifier’s relationship across all classes.

Our training approach is illustrated in Figure 2(a), and we provide a PyTorch-like pseudocode of it in Section B of the Appendix. It is important to note that we only use the class name to formulate the textual prompt l^p , and no other supplementary information such as class descriptions, concepts or hierarchies (see Section I in the Appendix for more information).

After training, the projected visual features and the text encoder features lie in the same space, and we can therefore query the visual features with any text by finding the alignment score between the encoded text and the visual features. In the case of image classification, the text queries remain the class prompts, and encoding them with the text encoder T is equivalent to generating the weights of a linear classifier for the newly formulated classification task, defined as $\text{argmax}(\tilde{f} \cdot U^T)$. This is shown in Figure 2(b).

4 Applications

In this section, we show how our method can be used to build text-based interpretability applications. At application, all model components (including the MLP) are frozen.

4.1 Zero-Shot Concept Bottleneck Models

Concept Bottleneck Models (CBMs) [1] are a class of inherently interpretable models and have recently attracted significant attention. They consist of two steps: (1) concept discovery, followed by (2) concepts-to-predictions. In step (1), the dense output features of a visual encoder are first mapped to textual concepts (e.g., words or short descriptions of objects) each with a score that represents the concept activation to the image. In step (2), a linear classifier W^{con} is trained on top of these concept activations to predict the class such that a prediction can be interpreted as a linear sum of interpretable concepts rather than a linear sum of opaque features. Recently, Label-Free CBMs (LF-CBMs) use CLIP to perform the concept discovery step without annotated image-concept data. This is achieved either by using CLIP as a model to provide ground-truth image-concept similarities to train a layer that performs concept discovery [15], or by querying the image features from a set of predefined concepts within the CLIP space [16, 17] and using the cosine similarity scores between the concepts and the image as concept activations. However, there are major limitations in this existing line of CBMs. Firstly, LF-CBMs are restricted to CLIP-based models, as the concept discovery step would otherwise not be possible since it necessitates an image-text similarity model. Secondly, all CBM approaches to date require training a linear probe on the concept activations, which 1) hinders an on-the-fly ready-to-deploy CBM at test-time directly, and 2) requires training a new W^{con} classifier from scratch for every different set of concepts, hindering flexibility to the choice of concepts.

Our method solves all the aforementioned issues, formulating zero-shot CBMs for any pretrained classifier. We remind readers from Section 3 that $U \in \mathbb{R}^{K \times m}$ is the output of the text encoder T for the class prompts, which in essence represent the classification weights of the newly formulated classifier. We assume that we are given a large set of predefined textual concepts, denoted as \mathcal{Z} , and with cardinality $|\mathcal{Z}| = Z$. Following other works [18], and without loss of generality, we use the $Z = 20K$ most common words in English [19] as our concept set. These are general concepts that are sufficiently expressive and represent world knowledge and are not tailored towards any specific dataset. To ensure that the concepts are meaningful, we apply a rigorous filtering procedure to the concept set. Specifically, we remove any terms that exactly match the target class name, as well as any constituent words that form the class name (for example, eliminating “tiger” and “shark” when the class name is “tiger shark”). In addition, we exclude terms corresponding to the parent and subparent classes (e.g., “fish” and “animal” for the class “tiger shark”), other species within the same category, and any synonyms of the target class name. This systematic filtering guarantees that the resulting concept set is free of terms that are overly similar or directly derived from the target classes.

We use the same text encoder T that generates the linear classifier U to generate concept embeddings, by feeding each concept $z_i \in \mathcal{Z}$ to the text encoder T to generate a concept embedding c_i . That is, $c_i = T(z_i)$, $\forall i = 1, \dots, Z$. By performing this for all Z concepts, we obtain a concept embedding matrix $C \in \mathbb{R}^{Z \times m}$. For an image I , we extract its visual features f and use the MLP to map them to \tilde{f} which now lies in the text embedding space. That is, $\tilde{f} = \text{MLP}(f)$, and $\tilde{f} \in \mathbb{R}^m$. Since C and the mapped visual features \tilde{f} are now in the same space, we can query \tilde{f} to find which concepts it responds to. That is, we perform concept discovery using the cosine similarity between \tilde{f} and each row-vector in C . The concept activations are obtained by $\tilde{f} \cdot C \in \mathbb{R}^Z$ and represent the activation score for each of the Z concepts. We provide an illustration in Figure 3(a).

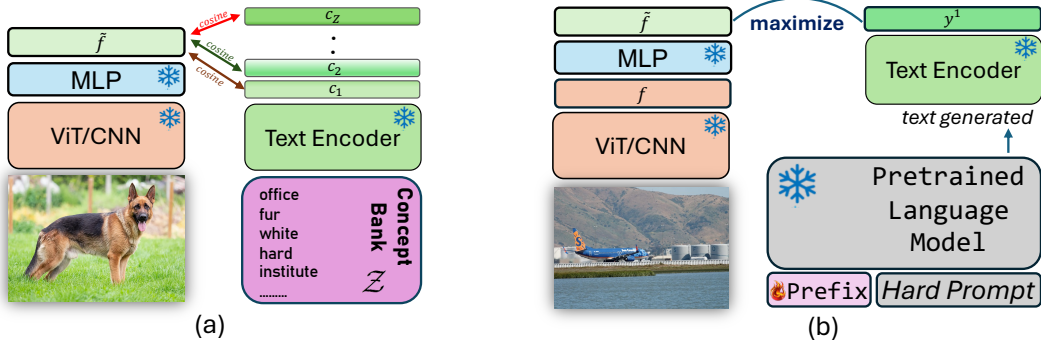


Figure 3: **(a)** Our approach to concept discovery in CBMs. **(b)** Decoding visual features into natural language using any pretrained language decoder (e.g., GPT-2). We apply prefix tuning while keeping the language decoder frozen, generating text that maximizes the similarity with the visual features. Shown for iteration $j = 1$

We now show how to build the classifier W^{con} that takes in the concept activations and outputs a distribution S_{cn} over classes. We build W^{con} in a zero-shot manner. Here, *zero-shot* indicates that no training is required to map concept activations to classes. Recall that both U and C are outputs of the text encoder T , and they are already in the same space. Therefore, we can build the weights of the classifier W^{con} with a text-to-text search between the concepts and the class name. Specifically, we calculate the cosine similarity between the concept embeddings C and the linear classifier U to obtain the new weights for W^{con} . That is, we perform $C \cdot U^T \in \mathbb{R}^{Z \times K}$. Therefore, the weights of W^{con} represent how similar the class name is to all the concepts. In total, the output distribution S_{cn} of the CBM is defined as:

$$S_{cn} = \underbrace{(\tilde{f} \cdot C^T)}_{\text{concept discovery}} \cdot \underbrace{(C \cdot U^T)}_{\text{concept-to-class}} = \tilde{f} \cdot \underbrace{C^T C}_{\text{gram matrix}} \cdot U^T. \quad (2)$$

From Eq. 2 we observe that we scale the linear feature-based classifier U by the gram matrix of concepts ($C^T C \in \mathbb{R}^{m \times m}$). Notably, if the gram matrix is identity ($C^T C = I$), we get back our original feature-based classifier given by $\tilde{f} \cdot U^T$. Therefore, to convert any classifier to a CBM, all we have to do is plug in the gram matrix in-between, making it a convenient way to directly switch to an

inherently interpretable model. Eq. 2 also shows that we do not change the linear classifier U , we only scale it by the gram matrix of concepts. This means our CBMs preserve the basis reasoning process of the original classifier. By this, we obtain zero-shot CBMs that discover concepts and builds W^{con} , both in a training-free manner and for any classifier. Note that our method is flexible in the concept set. The concept set is chosen at test time directly, and the CBM is built directly on-the-fly.

4.2 Zero-Shot Decoding of Visual Features into Text

In this application, we aim to decode the visual feature vector f for an image I , given by $f = F_v(I)$, into a natural language sentence. This offers a text-based interpretation of what the visual features contain. We adapt the method introduced in [3] for our purpose. Specifically, we first project the visual feature vector f using the MLP to obtain \tilde{f} . That is, $\tilde{f} = \text{MLP}(f)$. Since \tilde{f} is now in the same space as the text encoder T , we can measure its association to any encoded text. We utilize an off-the-shelf pretrained language decoder model (e.g., GPT-2), denoted as G , to generate open-ended text. We keep G frozen to maintain its language generation capabilities and instead use prefix-tuning [20] to guide G to generate a text that maximizes the similarity with the transformed visual feature vector \tilde{f} . Specifically, we attach a set of learnable “virtual” tokens to G . Denote the generated output text of G for one iteration as h^j , where j represents the iteration number. h^j is encoded with the text encoder T , to yield a vector y^j . That is, $y^j = T(h^j)$. As y^j and \tilde{f} are now in the same embedding space, we maximize the cosine similarity between them in order to update the learnable tokens. We perform this process for several iterations. An overview of this process is shown in Figure 3(b). As this process is not the core contribution of our work, we leave more details to Section H of the appendix, which also includes a detailed illustration in Figure 2.

5 Experiments

We first provide results on our newly formulated visual classifiers. We use the challenging ImageNet-1K dataset due to the widespread publicly available visual classifiers trained and evaluated on it. We apply our method on a diverse set of 40 visual classifiers. For CNNs, we consider the following family of models (each with several variants): Residual Networks (ResNets) [21], Wide ResNets [22], ResNeXts [23], ShuffleNetv2 [24], EfficientNetv2 [25], Densely Connected Networks (DenseNets) [26], ConvNeXts [27] and ConvNeXtv2 [28]. For Transformers, we consider the following family of models (each with several variants): Vision Transformers (ViTs) [29], DINOv2 [30], BEiT [31], the hybrid Convolution-Vision Transformer CvT [32], Swin Transformer [33] and Swin Transformer v2 [34]. All models are pretrained on ImageNet-1K from the PyTorch [35] and HuggingFace [36] libraries. Models with the subscript pt indicate that the model was pretrained on ImageNet-21k before being finetuned on ImageNet-1K. Models with a subscript $v2$ are trained following the updated PyTorch training recipe [37]. Finally, BEiT, DINOv2 and ConvNeXtv2 are pretrained in a self-supervised manner before being finetuned on ImageNet-1k. Both the pretrained classifier and text encoder remain frozen, only the MLP is trained on the ImageNet training set following Eq. 1.

Performance is evaluated using the same protocol and dataset splits as the original classifier, specifically the 50,000 validation split of ImageNet-1K. For the text encoder, we use the MiniLM Sentence Encoder [38], with ablation studies on other text encoders presented in Section D of the Appendix. Results are presented in Table 1. We report the replicated Top-1 accuracy of the re-formulated classifier with our method in the first column, the original Top-1 accuracy of the classifier in the second column, and the difference between them (Δ) in the last column. As can be seen, the loss in performance as indicated by Δ is minimal, with an average drop in performance of approximately 0.2 points across all models. We also perform ablation studies on the MLP to verify its effectiveness in Section C of the Appendix. We refer to Appendix Section F for results on other models and to Section G for implementation details.

Zero-Shot Concept Bottleneck Models: We report CBM evaluation results on the ImageNet validation set using the top-1 accuracy in Table 2. As baselines, we compare with 9 methods: LF-CBMs [15], LaBo [16], CDM [17], DCLIP [39], DN-CBMs [18], DCBM [40], Multi-Modal (MM) CBMs [41], CF-CBM [42] and SALF-CBM [43]. All these methods are supervised and use CLIP-based models either for computing the concept activations or as a backbone. Our zero-shot CBMs (ZS-CBMs) outperforms all the supervised CBMs and sets a new state-of-the-art. Notably, even a simple ResNet-50 classifier trained solely on ImageNet already outperforms the CBM for

Model	Top-1	Orig.	Δ	Model	Top-1	Orig.	Δ
ResNet50	75.80	76.13	-0.33	ResNeXt50-32x4d _{v2}	80.79	80.88	-0.09
ResNet50 _{v2}	80.14	80.34	-0.20	ResNeXt101-64x4d	83.13	83.25	-0.12
ResNet101 _{v2}	81.50	81.68	-0.18	ResNeXt101-32x8d	79.10	79.31	-0.21
ResNet101	77.19	77.37	-0.18	ViT-B/16	80.70	81.07	-0.37
WideResnet50	78.35	78.47	-0.12	ViT-B/16 _{v2}	84.94	85.30	-0.36
WideResNet50 _{v2}	81.17	81.31	-0.14	ViT-L/32	76.72	76.97	-0.25
WideResNet101 _{v2}	82.21	82.34	-0.13	ViT-L/16	79.56	79.66	-0.10
DenseNet161	77.04	77.14	-0.10	ViT-L/16 _{v2}	87.61	88.06	-0.45
DenseNet169	75.46	75.60	-0.14	Swin-Base	83.22	83.58	-0.36
EfficientNetv2-S	84.04	84.23	-0.19	Swinv2-Base	83.72	84.11	-0.39
EfficientNetv2-M	84.95	85.11	-0.16	BeiT-B/16	84.54	85.06	-0.52
ShuffleNetv2 _{x2.0}	75.83	76.23	-0.40	BeiT-L/16	87.22	87.34	-0.12
ConvNeXt-Small	83.42	83.62	-0.20	DINOv2-B	84.40	84.22	+0.18
ConvNeXt-Base	83.88	84.06	-0.18	ConvNeXtV2-B	84.56	84.73	-0.17
ConvNeXt-B _{pt}	85.27	85.52	-0.25	ConvNeXtV2-B _{pt}	86.07	86.25	-0.18
ResNeXt50-32x4d	77.44	77.62	-0.18	ConvNeXtV2-B _{pt} @384	87.34	87.50	-0.16

Table 1: Performance comparison of our re-formulated classifiers for several models. Top-1 indicates our results of the new formulation, and Orig. denotes the original Top-1 accuracy. Δ represents the difference between them ($\Delta = \text{Top-1} - \text{Orig.}$).

the significantly more powerful ResNet-50 CLIP model trained on 400M samples. The best results are obtained by the ConvNeXtV2 model, which achieve a top-1 accuracy of 86.4. All models show close to original accuracy, which means we can transform any classifier to be inherently interpretable without much loss in performance.

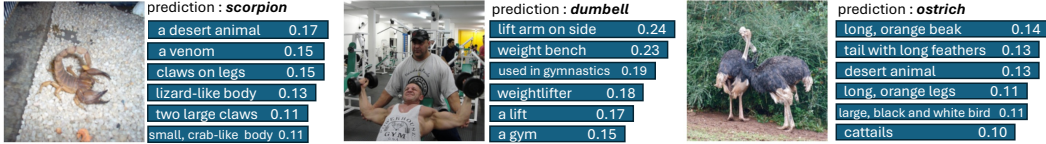


Figure 4: Qualitative examples of our zero-shot CBMs. We show the top-detected concepts, each with their corresponding importance score to the prediction.

Effectiveness of Concept Interventions: As a supplementary experiment, we also report concept intervention results on our ZS-CBMs in Section E of the Appendix, showing the effectiveness of the concepts, how we can mitigate biases, debug models and fix their reasoning by explicitly intervening in the concepts of the bottleneck layer to control predictions.

In Figure 4, we present qualitative examples of a selection from the top concepts responsible for the prediction, along with their weight importance. The weight importance is calculated by multiplying the concept activation with its corresponding weight to the predicted class. We use various concept sets to demonstrate the flexibility of our method to any desired concept set directly at test time (on-the-fly), as this process simply involves encoding the chosen concept set using the text encoder. All examples use the LF-CBM concept set [15]. By observing the first example, the image is predicted as a “scorpion” because it has a lizard-like overall body, it is a venomous, desert animal with claws on its legs, and has large claws on its hand that look like a crab. Interestingly, in the second example, the top-detected concept is a “lift arm on the side.” Although this is not the primary feature defining a dumbbell, it reflects a well-documented bias in the literature [44] regarding the “dumbbell” class. Because most training images for this class show a dumbbell being lifted by an arm, the classifier not only learns to recognize the dumbbell but also associates it with the hand or arm that lifts it. With our method, we can obtain a textual interpretation of the biases that the original classifier learns. We also provide qualitative examples of global class-wise concepts detected in Section K of the appendix.

Zero-Shot Decoding of Visual Features: We now evaluate the performance of the textually decoded visual features. Since the ground-truth content of visual features is unknown—that is, we do not know exactly what the model uses for reasoning—we rely on COCO captions [45] for evaluation. While these captions may not perfectly correspond to the actual information represented by a visual feature vector—potentially differing from what a human annotator expects—they provide a reasonable

Supervised CBMs					
Method	Model	Top-1	Method	Model	Top-1
LF-CBM	CLIP ResNet50	67.5	DN-CBM	CLIP ViT-B/16	79.5
LF-CBM	CLIP ViT-B/16	75.4	SALF-CBM-S	CLIP ViT-B/16	75.3
LaBo	CLIP ResNet50	68.9	SALF-CBM-D	CLIP ViT-B/16	76.3
LaBo	CLIP ViT-B/16	78.9	DCBM-SAM2	CLIP ViT-L/14	77.9
CDM	CLIP ResNet50	72.2	DCBM-GDINO	CLIP ViT-L/14	77.4
CDM	CLIP ViT-B/16	79.3	DCBM-RCNN	CLIP ViT-L/14	77.8
DCLIP	CLIP ViT-B/32	63.0	MM-CBM	CLIP ViT-B/16	77.9
DCLIP	CLIP ViT-B/16	68.0	MM-ProtoSim	CLIP ViT-B/16	78.8
DCLIP	CLIP ViT-L/14	75.0	CF-CBM-H	CLIP ViT-B/16	77.4
DN-CBM	CLIP ResNet50	72.9	CF-CBM-L	CLIP ViT-B/16	78.4
Zero-Shot CBMs (Ours)					
Method	Model	Top-1	Method	Model	Top-1
ZS-CBM	ResNet50	73.9	ZS-CBM	ViT-B/32	73.3
ZS-CBM	ResNet50 _{v2}	78.1	ZS-CBM	ViT-B/16	79.3
ZS-CBM	ResNet101	75.3	ZS-CBM	ViT-B/16 _{v2}	83.2
ZS-CBM	ResNet101 _{v2}	79.9	ZS-CBM	Swin-Base	82.2
ZS-CBM	WideResNet50	76.9	ZS-CBM	Swinv2-Base	82.6
ZS-CBM	WideResNet50 _{v2}	79.2	ZS-CBM	ViT-B/16 _{pt}	81.5
ZS-CBM	WideResNet101 _{v2}	81.0	ZS-CBM	BeiT-B/16	83.0
ZS-CBM	DenseNet121	69.9	ZS-CBM	DINOv2-B	82.6
ZS-CBM	DenseNet161	75.2	ZS-CBM	ConvNeXt-B _{pt}	84.0
ZS-CBM	EfficientNetv2-S	83.0	ZS-CBM	ConvNeXtV2-B _{pt}	84.9
ZS-CBM	EfficientNetv2-M	83.9	ZS-CBM	BeiT-L/16	86.2
ZS-CBM	ConvNeXt-Small	81.9	ZS-CBM	ViT-L/16 _{v2}	86.3
ZS-CBM	ConvNeXt-Base	82.8	ZS-CBM	ConvNeXtV2-B _{pt} @384	86.4

Table 2: Performance of Supervised and Zero-Shot CBMs on the ImageNet validation set.

approximation for this purpose, and represent the best available alternative for evaluation. Note that the COCO dataset differs in distribution than ImageNet, as a single image may contain many objects, interactions between them, and potentially categories not included in ImageNet (e.g., person). Therefore, it also serves as a way to evaluate generalization of our method to other datasets, given that we only used the ImageNet class names for training. Since we do not train any model on the ground-truth image captions provided by COCO, we use zero-shot image captioning as a benchmark.

We present results on the widely used “Karpathy test split” with various vision classifiers. As baselines, we compare our approach against existing methods in zero-shot image captioning, specifically ZeroCap [3] and ConZIC [46], both which use CLIP. For evaluation, we employ standard natural language generation metrics: BLEU-4 (B@4) [47], METEOR (M) [48], ROUGE-L (R-L) [49], CIDEr (C) [50], and SPICE (S) [51]. Results are shown in Table 3a. ConvNeXtv2 achieves state-of-the-art performance on CIDEr and SPICE, the two most critical metrics for evaluating image captioning systems. Even with a simple ResNet-50 vision encoder trained on ImageNet-1K (1.2 million images), our approach outperforms the baseline methods on CIDEr and SPICE, despite the latter utilizing the significantly more powerful CLIP vision encoder, trained on 400 million image-text pairs. We also present qualitative examples of the decoded visual features for different models in Figure 5. From the first example, BeiT-L/16 captures features of both the vegetables and the dog, whereas ConvNeXtV2 captures only the vegetables. In contrast, ViT-B/16 and DINOv2 focus exclusively on the dog and its characteristics. Although some generations lacks semantic correctness (e.g., who was born in a dog), they are still meaningful enough for humans to understand and reason. This application allows human-friendly interpretations of visual features, understandable even to a layman user.

Note that our results in Table 3a are outperformed by the baseline ZeroCap on the BLEU-4 (B4) and METEOR (M) metrics. However, it is important to note that B4 and M are n-gram overlap-based metrics. They assume that the generated caption follows a specific structure and style. We verify this by revisiting an old image captioning paradigm termed as *compositional captioning* [52], and later revived with deep learning methods [53]. In compositional captioning, a set of image-grounded concepts (such as attributes, objects and verbs) are first detected, and a language model is then used to compose them into a natural sounding sentence. With the current advancements of Large Language Models (LLMs), we can use an LLM as a compositor. Specifically, we detect the top concepts and

Model	B4	M	R-L	C	S	Model	B4	M	R-L	C	S
ZeroCap	2.6	11.5	—	14.6	5.5	ZeroCap	2.6	11.5	—	14.6	5.5
ConZIC	1.3	11.5	—	12.8	5.2	ConZIC	1.3	11.5	—	12.8	5.2
Ours						Ours					
DenseNet161	1.50	10.2	20.4	15.8	6.3	DenseNet161	4.20	12.5	30.1	17.0	6.6
ResNet50	1.43	10.2	20.3	15.9	6.2	ResNet50	4.10	12.5	30.1	17.0	6.6
WideResNet50	1.40	10.2	20.4	16.0	6.4	ResNet50 _{v2}	4.50	12.8	30.5	18.4	6.9
WideResNet101 _{v2}	1.50	10.4	20.5	16.6	6.4	WideResNet50 _{v2}	4.20	12.7	30.3	17.7	6.9
ResNet101 _{v2}	1.48	10.4	20.6	16.7	6.5	ResNet101 _{v2}	4.30	12.6	30.1	18.0	6.8
ResNet50 _{v2}	1.47	10.5	20.6	16.8	6.5	ConvNeXt-Base _{v2}	4.40	12.8	30.2	18.6	7.1
ConvNeXt-B _{pt}	1.50	10.6	20.8	17.2	6.7	ResNet50 _{v2}	4.50	12.8	30.5	18.4	6.9
DINOv2-Base	1.50	10.7	21.0	17.3	6.7	EfficientNetv2-S	4.40	12.7	30.4	18.6	6.9
ViT-B/16 _{v2}	1.50	10.5	20.9	17.3	6.5	ViT-B/16 _{pt}	4.50	12.8	30.2	18.7	7.2
BeiT-L/16	1.50	10.6	20.9	17.6	6.9	ConvNeXtV2-B _{pt} @384	4.40	12.7	30.2	18.7	7.2
ViT-B/16 _{pt}	1.50	10.7	20.9	17.7	6.9	BeiT-B/16	4.50	12.8	30.3	18.9	7.1
ConvNeXtV2-B _{pt} @384	1.60	10.7	21.1	17.9	6.9	DINOv2-Base	4.60	13.0	30.7	18.7	7.1

(a) Zero-Shot Image Captioning Performance

(b) Zero-Shot Compositional Captioning Performance

Table 3: Comparison of Zero-Shot Captioning Performance

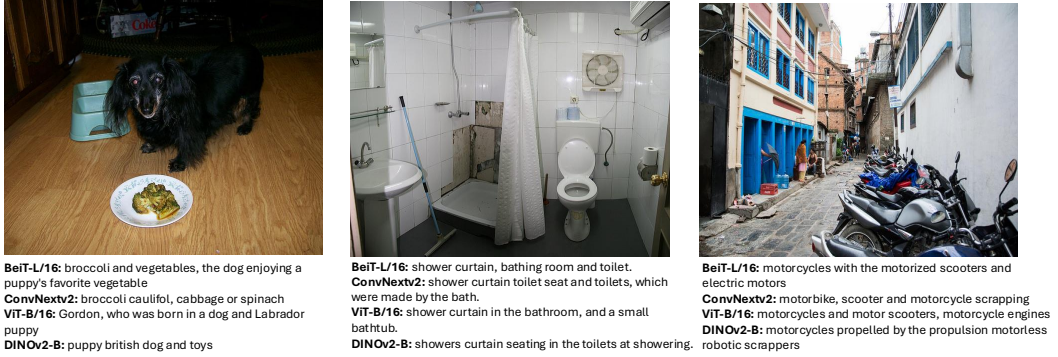


Figure 5: Qualitative examples of decoded visual features from different visual classifiers, into text.

verbs to the image using the concept discovery method introduced in Section 4.1 and shown in Figure 3(a), and feed them, along with their similarity scores, to an LLM. For the concepts, we use the same concept set as in Section 4.1. We also add a list of the most common verbs [54] in English to the pool. This allows us to cover all possible words and interactions. We prompt the LLM to utilize the provided information to compose a sentence, given a very few in-context examples from the COCO captioning training set (in our experiments, we use 9 examples). This allows us to generate sentences adhering to a specific style and structure. For this experiment, we used GPT4o-mini [55] as our LLM, as it is fast and cost-efficient. In the prompt, we explicitly instruct the LLM to refrain from reasoning or generating content based on its own knowledge or assumptions, and that all its outputs must be strictly grounded in the provided concepts, verbs, and score importances. We provide details on the exact prompt we used in Appendix Section J. Results are shown in Table 3b. While results on CiDER and SPICE are incremental compared to results in Table 3a, the n-gram metrics (B4, M and R-L) are boosted, which verifies our hypothesis about the low scores of B4 and M in Table 3a compared to baseline methods. Also note that, since the LLM is generic and can adapt to any style and structure, compositional captioning is especially useful for generating captions tailored to specific domains (see Section J.1 in the appendix).

6 Conclusion

We presented a method to transform visual classifiers such that they can be queried via open-set text queries. We achieve state-of-the-art results in two applications, i.e., zero-shot CBMs and decoding of visual features into natural language sentences. Our method can be applied to various other applications that were previously restricted to CLIP models. Our work removes this restriction, being applicable to any visual classifier. Finally, as with any research work, this study has its own limitations which are discussed in Appendix Section A.

References

- [1] Pang Wei Koh, Thao Nguyen, Yew Siang Tang, Stephen Mussmann, Emma Pierson, Been Kim, and Percy Liang. Concept bottleneck models. In *Proceedings of the 37th International Conference on Machine Learning*, pages 5338–5348, 2020.
- [2] Tuomas Oikarinen and Tsui-Wei Weng. CLIP-dissect: Automatic description of neuron representations in deep vision networks. In *The Eleventh International Conference on Learning Representations*, 2023.
- [3] Yoad Tewel, Yoav Shalev, Idan Schwartz, and Lior Wolf. Zerocap: Zero-shot image-to-text generation for visual-semantic arithmetic. *2022 IEEE/CVF Conference on Computer Vision and Pattern Recognition (CVPR)*, pages 17897–17907, 2021.
- [4] Alec Radford, Jong Wook Kim, Chris Hallacy, Aditya Ramesh, Gabriel Goh, Sandhini Agarwal, Girish Sastry, Amanda Askell, Pamela Mishkin, Jack Clark, Gretchen Krueger, and Ilya Sutskever. Learning transferable visual models from natural language supervision. In *International Conference on Machine Learning (ICML)*, 2021.
- [5] Yuhui Zhang, Alyssa Unell, Xiaohan Wang, Dhruba Ghosh, Yuchang Su, Ludwig Schmidt, and Serena Yeung-Levy. Why are visually-grounded language models bad at image classification? In *The Thirty-eighth Annual Conference on Neural Information Processing Systems*, 2024.
- [6] Jia Deng, Wei Dong, Richard Socher, Li-Jia Li, K. Li, and Li Fei-Fei. Imagenet: A large-scale hierarchical image database. *2009 IEEE Conference on Computer Vision and Pattern Recognition*, pages 248–255, 2009.
- [7] Meghal Dani, Isabel Rio-Torto, Stephan Alaniz, and Zeynep Akata. Devil: Decoding vision features into language. *German Conference on Pattern Recognition (GCPR)*, 2023.
- [8] Jack Merullo, Louis Castricato, Carsten Eickhoff, and Ellie Pavlick. Linearly mapping from image to text space. In *The Eleventh International Conference on Learning Representations*, 2023.
- [9] Dong Huk Park, Lisa Anne Hendricks, Zeynep Akata, Anna Rohrbach, Bernt Schiele, Trevor Darrell, and Marcus Rohrbach. Multimodal explanations: Justifying decisions and pointing to the evidence. *2018 IEEE/CVF Conference on Computer Vision and Pattern Recognition (CVPR)*, pages 8779–8788, 2018.
- [10] Maxime Kayser, Oana-Maria Camburu, Leonard Salewski, Cornelius Emde, Virginie Do, Zeynep Akata, and Thomas Lukasiewicz. e-vil: A dataset and benchmark for natural language explanations in vision-language tasks. *2021 IEEE/CVF International Conference on Computer Vision (ICCV)*, pages 1224–1234, 2021.
- [11] Fawaz Sammani, Tanmoy Mukherjee, and Nikos Deligiannis. Nlx-gpt: A model for natural language explanations in vision and vision-language tasks. *2022 IEEE/CVF Conference on Computer Vision and Pattern Recognition (CVPR)*, pages 8312–8322, 2022.
- [12] Leonard Salewski, A. Sophia Koepke, Hendrik P. A. Lensch, and Zeynep Akata. Zero-shot translation of attention patterns in vqa models to natural language. In *DAGM*, 2023.
- [13] Mazda Moayeri, Keivan Rezaei, Maziar Sanjabi, and Soheil Feizi. Text-to-concept (and back) via cross-model alignment. In *International Conference on Machine Learning*, 2023.
- [14] Sriram Balasubramanian, Samyadeep Basu, and Soheil Feizi. Decomposing and interpreting image representations via text in vits beyond CLIP. In *The Thirty-eighth Annual Conference on Neural Information Processing Systems*, 2024.
- [15] Tuomas Oikarinen, Subhro Das, Lam M. Nguyen, and Tsui-Wei Weng. Label-free concept bottleneck models. In *The Eleventh International Conference on Learning Representations*, 2023.

[16] Yue Yang, Artemis Panagopoulou, Shenghao Zhou, Daniel Jin, Chris Callison-Burch, and Mark Yatskar. Language in a bottle: Language model guided concept bottlenecks for interpretable image classification. *2023 IEEE/CVF Conference on Computer Vision and Pattern Recognition (CVPR)*, pages 19187–19197, 2022.

[17] Konstantinos P. Panousis, Dino Ienco, and Diego Marcos. Sparse linear concept discovery models. *2023 IEEE/CVF International Conference on Computer Vision Workshops (ICCVW)*, pages 2759–2763, 2023.

[18] Sukrut Rao, Sweta Mahajan, Moritz Bohle, and Bernt Schiele. Discover-then-name: Task-agnostic concept bottlenecks via automated concept discovery. In *European Conference on Computer Vision*, 2024.

[19] Google. google-10000-english, 2016. URL <https://github.com/first20hours/google-10000-english>.

[20] Xiang Lisa Li and Percy Liang. Prefix-tuning: Optimizing continuous prompts for generation. *Proceedings of the 59th Annual Meeting of the Association for Computational Linguistics and the 11th International Joint Conference on Natural Language Processing (Volume 1: Long Papers)*, pages 4582–4597, 2021.

[21] Kaiming He, X. Zhang, Shaoqing Ren, and Jian Sun. Deep residual learning for image recognition. *2016 IEEE Conference on Computer Vision and Pattern Recognition (CVPR)*, pages 770–778, 2015.

[22] Sergey Zagoruyko and Nikos Komodakis. Wide residual networks. In *BMVC*, 2016.

[23] Saining Xie, Ross B. Girshick, Piotr Dollár, Zhuowen Tu, and Kaiming He. Aggregated residual transformations for deep neural networks. *2017 IEEE Conference on Computer Vision and Pattern Recognition (CVPR)*, pages 5987–5995, 2016.

[24] Ningning Ma, Xiangyu Zhang, Hai-Tao Zheng, and Jian Sun. Shufflenet v2: Practical guidelines for efficient cnn architecture design. In *Proceedings of the European Conference on Computer Vision (ECCV)*, September 2018.

[25] Mingxing Tan and Quoc V. Le. Efficientnetv2: Smaller models and faster training. In *International Conference on Machine Learning (ICML)*, 2021.

[26] Gao Huang, Zhuang Liu, and Kilian Q. Weinberger. Densely connected convolutional networks. *2017 IEEE Conference on Computer Vision and Pattern Recognition (CVPR)*, pages 2261–2269, 2016.

[27] Zhuang Liu, Hanzi Mao, Chaozheng Wu, Christoph Feichtenhofer, Trevor Darrell, and Saining Xie. A convnet for the 2020s. *2022 IEEE/CVF Conference on Computer Vision and Pattern Recognition (CVPR)*, pages 11966–11976, 2022.

[28] Sanghyun Woo, Shoubhik Debnath, Ronghang Hu, Xinlei Chen, Zhuang Liu, In-So Kweon, and Saining Xie. Convnext v2: Co-designing and scaling convnets with masked autoencoders. *2023 IEEE/CVF Conference on Computer Vision and Pattern Recognition (CVPR)*, pages 16133–16142, 2023.

[29] Alexey Dosovitskiy, Lucas Beyer, Alexander Kolesnikov, Dirk Weissenborn, Xiaohua Zhai, Thomas Unterthiner, Mostafa Dehghani, Matthias Minderer, Georg Heigold, Sylvain Gelly, Jakob Uszkoreit, and Neil Houlsby. An image is worth 16x16 words: Transformers for image recognition at scale. In *International Conference on Learning Representations (ICLR)*, 2021.

[30] Maxime Oquab, Timothée Darcet, Théo Moutakanni, Huy V. Vo, Marc Szafraniec, Vasil Khalidov, Pierre Fernandez, Daniel HAZIZA, Francisco Massa, Alaaeldin El-Nouby, Mido Assran, Nicolas Ballas, Wojciech Galuba, Russell Howes, Po-Yao Huang, Shang-Wen Li, Ishan Misra, Michael Rabbat, Vasu Sharma, Gabriel Synnaeve, Hu Xu, Herve Jegou, Julien Mairal, Patrick Labatut, Armand Joulin, and Piotr Bojanowski. DINOv2: Learning robust visual features without supervision. *Transactions on Machine Learning Research*, 2024. ISSN 2835-8856.

[31] Hangbo Bao, Li Dong, Songhao Piao, and Furu Wei. BEit: BERT pre-training of image transformers. In *International Conference on Learning Representations*, 2022.

[32] Haiping Wu, Bin Xiao, Noel C. F. Codella, Mengchen Liu, Xiyang Dai, Lu Yuan, and Lei Zhang. Cvt: Introducing convolutions to vision transformers. *2021 IEEE/CVF International Conference on Computer Vision (ICCV)*, pages 22–31, 2021.

[33] Ze Liu, Yutong Lin, Yue Cao, Han Hu, Yixuan Wei, Zheng Zhang, Stephen Lin, and Baining Guo. Swin transformer: Hierarchical vision transformer using shifted windows. *2021 IEEE/CVF International Conference on Computer Vision (ICCV)*, pages 9992–10002, 2021.

[34] Ze Liu, Han Hu, Yutong Lin, Zhuliang Yao, Zhenda Xie, Yixuan Wei, Jia Ning, Yue Cao, Zheng Zhang, Li Dong, Furu Wei, and Baining Guo. Swin transformer v2: Scaling up capacity and resolution. *2022 IEEE/CVF Conference on Computer Vision and Pattern Recognition (CVPR)*, pages 11999–12009, 2021.

[35] TorchVision maintainers and contributors. Torchvision: Pytorch’s computer vision library. <https://github.com/pytorch/vision>, 2016.

[36] Thomas Wolf, Lysandre Debut, Victor Sanh, Julien Chaumond, Clement Delangue, Anthony Moi, Pierrick Cistac, Tim Rault, Rémi Louf, Morgan Funtowicz, Joe Davison, Sam Shleifer, Patrick von Platen, Clara Ma, Yacine Jernite, Julien Plu, Canwen Xu, Teven Le Scao, Sylvain Gugger, Mariama Drame, Quentin Lhoest, and Alexander M. Rush. Transformers: State-of-the-art natural language processing. In *Proceedings of the 2020 Conference on Empirical Methods in Natural Language Processing: System Demonstrations*, pages 38–45, Online, October 2020. Association for Computational Linguistics. URL <https://www.aclweb.org/anthology/2020.emnlp-demos.6>.

[37] Vasilis Vryniotis. How to train state-of-the-art models using torchvision’s latest primitives, 2021. URL <https://pytorch.org/blog/how-to-train-state-of-the-art-models-using-torchvision-latest-primitives/>.

[38] Wenhui Wang, Furu Wei, Li Dong, Hangbo Bao, Nan Yang, and Ming Zhou. Minilm: Deep self-attention distillation for task-agnostic compression of pre-trained transformers, 2020.

[39] Sachit Menon and Carl Vondrick. Visual classification via description from large language models. *International Conference on Learning Representations*, 2023.

[40] Patrick Knab, Katharina Prasse, Sascha Marton, Christian Bartelt, and Margret Keuper. Dcbm: Data-efficient visual concept bottleneck models. 2024.

[41] Fawaz Sammani and Nikos Deligiannis. Interpreting and analysing CLIP’s zero-shot image classification via mutual knowledge. In *The Thirty-eighth Annual Conference on Neural Information Processing Systems*, 2024.

[42] Konstantinos P. Panousis, Dino Ienco, and Diego Marcos. Coarse-to-fine concept bottleneck models. In *The Thirty-eighth Annual Conference on Neural Information Processing Systems*, 2024.

[43] Itay Benou and Tammy Riklin-Raviv. Show and tell: Visually explainable deep neural nets via spatially-aware concept bottleneck models. *2025 IEEE Conference on Computer Vision and Pattern Recognition (CVPR)*, 2025.

[44] Wojciech Samek and Klaus-Robert Müller. Towards explainable artificial intelligence. *ArXiv*, abs/1909.12072, 2019. URL <https://api.semanticscholar.org/CorpusID:202579608>.

[45] Tsung-Yi Lin, Michael Maire, Serge J. Belongie, James Hays, Pietro Perona, Deva Ramanan, Piotr Dollár, and C. Lawrence Zitnick. Microsoft coco: Common objects in context. In *European Conference on Computer Vision*, 2014.

[46] Zequn Zeng, Hao Zhang, Zhengjue Wang, Ruiying Lu, Dongsheng Wang, and Bo Chen. Conzic: Controllable zero-shot image captioning by sampling-based polishing. *2023 IEEE/CVF Conference on Computer Vision and Pattern Recognition (CVPR)*, pages 23465–23476, 2023.

[47] Kishore Papineni, Salim Roukos, Todd Ward, and Wei-Jing Zhu. Bleu: a method for automatic evaluation of machine translation. In *Annual Meeting of the Association for Computational Linguistics*, 2002.

[48] Satanjeev Banerjee and Alon Lavie. Meteor: An automatic metric for mt evaluation with improved correlation with human judgments. In *IEEvaluation@ACL*, 2005.

[49] Chin-Yew Lin. ROUGE: A package for automatic evaluation of summaries. In *Text Summarization Branches Out*, pages 74–81, Barcelona, Spain, July 2004. Association for Computational Linguistics. URL <https://aclanthology.org/W04-1013/>.

[50] Ramakrishna Vedantam, C. Lawrence Zitnick, and Devi Parikh. Cider: Consensus-based image description evaluation. *2015 IEEE Conference on Computer Vision and Pattern Recognition (CVPR)*, pages 4566–4575, 2014.

[51] Peter Anderson, Basura Fernando, Mark Johnson, and Stephen Gould. Spice: Semantic propositional image caption evaluation. In *Computer Vision–ECCV 2016: 14th European Conference, Amsterdam, The Netherlands, October 11–14, 2016, Proceedings, Part V 14*, pages 382–398. Springer, 2016.

[52] Girish Kulkarni, Visruth Premraj, Sagnik Dhar, Siming Li, Yejin Choi, Alexander C. Berg, and Tamara L. Berg. Baby talk: Understanding and generating simple image descriptions. *CVPR 2011*, pages 1601–1608, 2011.

[53] Jiasen Lu, Jianwei Yang, Dhruv Batra, and Devi Parikh. Neural baby talk. *2018 IEEE/CVF Conference on Computer Vision and Pattern Recognition*, pages 7219–7228, 2018.

[54] Manh Dat. List of all english words (common), 2015. URL <https://github.com/datmt/English-Words-Updated>.

[55] OpenAI. Gpt-4o mini: advancing cost-efficient intelligence, 2024. URL <https://openai.com/index/gpt-4o-mini-advancing-cost-efficient-intelligence/>.

[56] Bolei Zhou, Agata Lapedriza, Aditya Khosla, Aude Oliva, and Antonio Torralba. Places: A 10 million image database for scene recognition. *IEEE Transactions on Pattern Analysis and Machine Intelligence*, 2017.

[57] Mitchell Wortsman, Gabriel Ilharco, Mike Li, Jong Wook Kim, Hannaneh Hajishirzi, Ali Farhadi, Hongseok Namkoong, and Ludwig Schmidt. Robust fine-tuning of zero-shot models. *2022 IEEE/CVF Conference on Computer Vision and Pattern Recognition (CVPR)*, pages 7949–7961, 2021.

[58] Nils Reimers and Iryna Gurevych. Sentence-bert: Sentence embeddings using siamese bert networks. In *Proceedings of the 2019 Conference on Empirical Methods in Natural Language Processing*. Association for Computational Linguistics, 11 2019.

[59] Shiori Sagawa*, Pang Wei Koh*, Tatsunori B. Hashimoto, and Percy Liang. Distributionally robust neural networks. In *International Conference on Learning Representations*, 2020.

[60] Jeremy Howard. Imagenette: A smaller subset of 10 easily classified classes from imagenet, March 2019.

[61] Jimmy Ba, Jamie Ryan Kiros, and Geoffrey E. Hinton. Layer normalization. *ArXiv*, abs/1607.06450, 2016.

[62] Dan Hendrycks and Kevin Gimpel. Gaussian error linear units (gelus). *arXiv: Learning*, 2016.

[63] Nitish Srivastava, Geoffrey E. Hinton, Alex Krizhevsky, Ilya Sutskever, and Ruslan Salakhutdinov. Dropout: a simple way to prevent neural networks from overfitting. *J. Mach. Learn. Res.*, 15:1929–1958, 2014.

[64] Diederik Kingma and Jimmy Ba. Adam: A method for stochastic optimization. In *International Conference on Learning Representations (ICLR)*, San Diego, CA, USA, 2015.

- [65] Ilya Loshchilov and Frank Hutter. SGDR: Stochastic gradient descent with warm restarts. In *International Conference on Learning Representations*, 2017.
- [66] Dekang Lin. Wordnet: An electronic lexical database. 1998.
- [67] Sarah Pratt, Rosanne Liu, and Ali Farhadi. What does a platypus look like? generating customized prompts for zero-shot image classification. *International Conference on Computer Vision (ICCV)*, 2023.
- [68] Robin Rombach, Andreas Blattmann, Dominik Lorenz, Patrick Esser, and Björn Ommer. High-resolution image synthesis with latent diffusion models. In *Proceedings of the IEEE/CVF Conference on Computer Vision and Pattern Recognition (CVPR)*, pages 10684–10695, June 2022.

A Limitations

As with any research work, our study has its own limitations that should be transparent and acknowledged. In particular, we identify two primary limitations of our method: the first concerns wrong semantic associations of class names in CBMs, while the second pertains to the limited generalization of our method to fine-grained datasets.

We start by addressing the first limitation of wrong semantic associations of class names in CBMs. This issue is closely tied to the choice of concept set used. When using the 20K most common words in English as our concept set, we observe that class names get associated to wrong semantically-related concepts. Figure 1 illustrates such cases. In the first example, the bird drake is linked to artist-related concepts (Rihanna, Robbie, lyric). This occurs because the bird “drake” is less familiar to the text encoder than the artist “drake”. In fact, a google search with the word “drake” yields directly the artist rather than the bird. In the second example, the top-detected concepts for the prediction “african grey” are incorrect semantic associations with the word “african” (ethiopian, tanzania) and the word “grey” (purple, blue) that do not pertain to the bird itself. We also observe similar cases that may raise ethical concerns (e.g., the animal “cock” leads to associations with male reproductive terms). For each example, we also report the total logit score of the prediction.

However, it is worth noting the following:

1. Meaningful concepts such as “duck” (first example) are still detected among the top concepts.
2. The incorrect semantic associations contribute only a negligible portion of the total logit, accounting for approximately 0.01% of the overall prediction score.
3. This issue is considerably less severe when using alternative concept sets, such as the LF-CBM concept set tailored for ImageNet.
4. This issue also appears in CLIP-based CBMs and hence not unique to our approach.

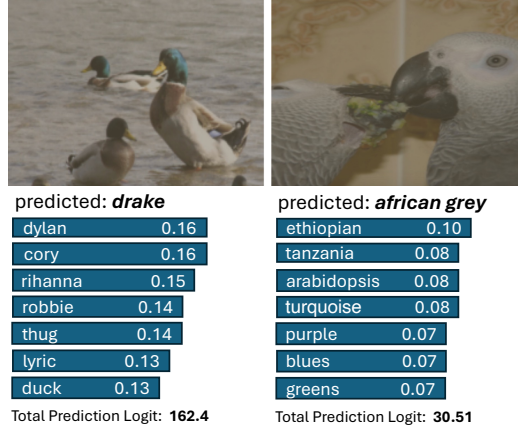


Figure 1: Limitations of our method is wrong semantic concept association in CBMs

The second limitation is the lack of generalization to fine-grained datasets. We test our ImageNet-trained reformulated classifiers to perform zero-shot transfer to the Places365 dataset [56] for scene classification. It is important to note that Places365 is known to induce low performance, even when using supervised training with the powerful CLIP model, making it a challenging classification dataset. To perform zero-shot transfer, we convert the class names of Places365 into text prompts of the form: “a scene of a {class} location” which are then encoded using the text encoder T to obtain the classification weights U_{places} . The image is encoded with the respective vision encoder to obtain the visual features f , which are then projected via the MLP to yield \tilde{f} . Zero-shot classification is performed using $\text{argmax}(\tilde{f} \cdot U_{places}^T)$. Results on the Places365 validation set are shown in Table 1. We report the supervised learning performance by training a linear probe on top of the CLIP model features. The supervised top-1 accuracy is 53.40 and 55.10 for ResNet50 and ViT-B/16 CLIP models, respectively. As demonstrated, these low top-1 accuracies suggest that Places365 is a particularly challenging dataset for classification. We then report the zero-shot performance of our method on

several visual classifiers. The best-performing model achieves a top-1 zero-shot accuracy of 14.36%, much lower than the supervised performance.

However, we emphasize that the observed low generalization performance **is not attributed to our formulation**; rather, it stems from the inherent limitations of the classifier itself. If the classifier (e.g., ResNet101) fails to generalize to out-of-distribution (OOD) fine-grained classes—as is the case—then it is unreasonable to expect the text-transformed classifier to perform any better. Since our transformed classifier is a replication of the original classifier, it inherits all of its limitations. In fact, expecting improved performance from the transformed classifier would be counterintuitive, as it would indicate a departure from the original classifier’s underlying reasoning. Moreover, as demonstrated in Table 1, models that benefit from large-scale pretraining tend to achieve superior OOD fine-grained performance, a trend that is consistent with findings in the OOD literature [57]. Finally, our approach performs significantly better than a randomly shuffled classifier where we shuffle its weights across classes.

Model	Top-1 (%)	Top-5 (%)
Supervised		
CLIP RN50 Linear Probe	53.40	-
CLIP ViT-B Linear Probe	55.10	-
Zero-Shot		
Shuffled Classifier	0.24	1.54
DenseNet161	10.55	25.18
ResNet50	10.58	25.14
ResNet101	10.97	25.42
ViT-B/16	11.47	26.53
ResNet50v2	11.66	27.40
ConvNeXt-Base	11.76	27.12
Swin-Base	12.12	26.83
Swinv2-Base	12.13	27.18
EfficientNetv2-M	12.31	28.33
ViT-B/16v2	13.11	29.54
DINOv2-Base	13.96	32.35
ConvNeXtv2 (pt)	14.05	30.92
BeiT-L/16	14.15	31.08
ViT-B/16 (pt)	14.22	32.18
ConvNeXt (pt)	14.36	31.64

Table 1: Top-1 and Top-5 zero-shot transfer results to Places365 for various models

B Pseudocode of our method

We provide a PyTorch-like pseudocode of our training approach in Listing 1.

```

# text_feats: textual features of class names from a frozen sentence encoder, shape (num_classes, text_dim)
# classifier: linear classifier weights of a frozen vision_encoder, shape (visual_dim, num_classes)
# mlp: trainable MLP from visual_dim -> text_dim
# images: batch of B images, shape (N, 3, height, width)

visual_feats = vision_encoder(images) # (N, visual_dim)
logits = visual_feats @ classifier # (N, num_classes)
original_dist = softmax(logits, dim=-1) # (N, num_classes)

mapped_feats = mlp(visual_feats) # (N, text_dim)
mapped_feats = l2_norm(mapped_feats) # (N, text_dim)
text_feats = l2_norm(text_feats) # (N, text_dim)

pred_logits = mapped_feats @ text_feats.T # (N, num_classes)
pred_dist = softmax(pred_logits, dim=-1) # (N, num_classes)

# cross entropy with original model's soft distribution
loss = -(original_dist * log(pred_dist)).sum(dim=1).mean()
loss.backward() # only mapper parameters are updated

```

Listing 1: PyTorch-like pseudocode for our method

C Ablation Studies of the MLP

In this section, we evaluate the impact of the MLP and verify its effectiveness. We perform the following ablation studies: **1) Mean Ablation:** For an image, we replace the input features to the MLP with a constant mean of the features calculated across the full ImageNet validation set. **2) Random Features:** For an image, we replace the input features to the MLP with random values sampled from a normal distribution with a mean and standard deviation equal to that of the features calculated across the full ImageNet validation set. **3) Random Weight Ablation:** We randomize the weights of the MLP projection. **4) Shuffled Ablation:** For an image, we replace the input features to the MLP with input features of another random image in the validation dataset.

For each ablation experiment, we compute the ImageNet validation accuracy. We expect the accuracy to drop across all ablations. As shown in Table 2, the accuracy nearly drops to zero in every case, confirming the effectiveness of our MLP.

Model		Mean Feature ↓	Random Features ↓	Shuffled Features ↓	Random Weights ↓
ResNet101v2	Ours	81.49	81.49	81.49	81.49
	Ablated	0.10	0.11	1.70	0.11
ConvNeXt-Base	Ours	83.88	83.88	83.88	83.88
	Ablated	0.10	0.11	1.79	0.10
BeiT-L/16	Ours	87.22	87.22	87.22	87.22
	Ablated	0.10	0.11	1.87	0.11
DINOv2-B	Ours	84.40	84.40	84.40	84.40
	Ablated	0.10	0.13	1.76	0.09

Table 2: Ablation studies of the MLP.

D Ablation Studies on the Text Encoder

In Table 3, we present ablation studies using other text encoders from the Sentence-BERT library [58] with the ResNet50 visual classifier. We observe that the choice of the text encoder has minimal effect on the performance. This is because even lower-performing text encoders are capable of understanding class names.

Text Encoder	Top-1 (%)
DistilRoberta	75.73
MPNet-Base	75.78
MPNet-Base-MultiQA	75.76
MinILM	75.80

Table 3: Ablation studies on other text encoders

E Effectiveness of Concept Interventions

As a supplementary experiment, we also report concept intervention results on our ZS-CBMs. Interventions on CBMs are an effective tool to mitigate biases, debug models and fix their reasoning by explicitly intervening in the concepts of the bottleneck layer to control predictions. The Waterbirds-100 dataset [59] is a standard dataset used in previous works [18] to conduct CBM intervention experiments. It is a binary classification dataset of two classes: waterbirds and landbirds. The training images of waterbirds are on water backgrounds, and training images of landbirds are on land backgrounds. However, the validation images do not have that correlation, where waterbird images appear on land backgrounds and landbird images on water backgrounds. The model is assumed to learn the water–land background correlation to perform this classification task. By building a CBM, we can correct this bias by intervening in concepts in the CB layer. However, there are two challenges associated with using the Waterbirds dataset in our work, and therefore we curated a validation dataset of waterbirds/landbirds directly from the ImageNet validation set. We provide more details about this process in Section L. Our curated dataset includes 140 validation images (70 for each class).

We create our ZS-CBM using the two class prompts: “an image of a waterbird” (for the waterbird class) and “an image of a landbird” (for the landbird class), and using the same concept set from [18] which includes a collection of bird-related concepts and a collection of land-related concepts. The ZS-CBM achieves a low accuracy, as shown in Table 4, which indicates the water-land bias the model performs for classification. To correct this, we intervene in the concepts in the CB layer, following the setup from [18]. **Intervention R (Int. R):** We zero-out activations of any bird concepts from the bottleneck layer, and expect the accuracy to drop. **Intervention K (Int. K):** We keep activations of bird concepts as they are, but scale down the activations of all remaining concepts by multiplying them with a factor of 0.1, and expect the accuracy to increase. Results are presented in Table 4 for some models, and demonstrate the success of our intervention experiments.

We also conduct concept intervention experiments with a more challenging multi-class setup. Unlike the Waterbirds dataset where bias-correlation issues are assumed, we make no such assumption here. We instead evaluate whether intervening on class-related concepts in the bottleneck layer and zeroing out their activations, impairs model accuracy. A drop in accuracy indicates that these concepts are important for prediction. We select a subset of 10 classes from ImageNet following [60]. We use the original ImageNet validation images for those classes, rather than the validation set from [60], because the latter contains original ImageNet training examples that our model has already seen. We employ an LLM to generate 5 highly-relevant concepts for each class, achieving in total 50 concepts. The classes and concepts we used are provided in Section M of the supplementary material. We then measure CBM accuracy before and after intervention. Results are provided in Table 5. For each image, we zero out the activations of its class-related concepts and report the **Intervention R (Int. R)** metric. As shown in Table 5, this intervention reduces accuracy by approximately 20% on average, underscoring the concepts importance to the CBM.

Model	Orig. CBM	Int. (R)↓	Int. (K)↑
BeiT-B/16	54.29	41.43 (-12.86)	58.57 (+4.28)
ConvNeXtV2 _{pt} @384	53.57	42.14 (-11.43)	59.29 (+5.72)
ConvNeXt_B _{pt}	53.57	42.86 (-10.71)	58.57 (+5.00)
DiNOv2	52.86	43.57 (-9.29)	59.29 (+6.43)
BeiT-L/16	52.86	44.29 (-8.57)	58.57 (+5.71)

Table 4: CBM Interventions on the standard Waterbirds dataset

Model	Orig. CBM	Int. (R)↓
ResNet50	96.80	76.00 (-20.8)
ResNet101	97.00	76.80 (-20.2)
DiNOv2-B	98.60	78.40 (-20.2)
BeiT-B/16	98.60	78.80 (-19.8)
ConvNeXtV2 _{pt} @384	99.40	79.40 (-20.0)

Table 5: CBM Interventions in a multi-class setup

F Performance on Additional Models

We report performance on additional models that were not included in the main manuscript in Table 6.

G Implementation Details

For the text encoder, we use the all-MiniLM-L12-v1² model available on the Sentence Transformers library [58]. This text encoder was trained on a large and diverse dataset of over 1 billion training text pairs. It contains a dimensionality of $m = 384$ and has a maximum sequence length of 256.

²<https://huggingface.co/sentence-transformers/all-MiniLM-L12-v1>

Model	Top-1	Orig.	Δ
ConvNeXt-Tiny	82.19	82.52	-0.33
ViT-B/32	75.40	75.91	-0.51
Swin-Small	82.63	83.20	-0.57
Swinv2-Tiny	81.44	82.07	-0.63
CvT-21	80.45	81.27	-0.82
Swinv2-Small	83.32	83.71	-0.39
ViT-B/16 _{pt}	83.55	84.37	-0.82

Table 6: Performance of our reformulated classifiers for additional models

Our MLP projector is composed of 3 layers, the first projects the visual feature dimensions n to $n \times 2$ and is followed by a Layer Normalization [61], a GELU activation function [62] and Dropout [63] with a drop probability of 0.5. The second layer projects the $n \times 2$ dimensions to $n \times 2$ and is followed by a Layer Normalization and a GELU activation function. The final linear layer projects the $n \times 2$ dimensions to m (the dimensions of the text encoder). We train the MLP projector with a batch size of 256 using the ADAM optimizer [64] with a learning rate of 1e-4 that decays using a cosine schedule [65] over the total number of epochs. We follow the original image sizes that the classifier was trained on.

For the training images, we apply the standard image transformations that all classifiers were trained on which include a Random Resized Crop and a Random Horizontal Flip. For the validation images, we follow exactly the transformations that the classifier was evaluated on, which include resizing the image followed by a Center Crop to the image size that the classifier expects. Each model is trained on a single NVIDIA GeForce RTX 2080 Ti GPU.

H Process of Decoding Visual Features

We remind readers of the mapping function, denoted as MLP, that transforms the visual features f into the same space as textual features, producing \tilde{f} . A pre-trained language model G is then optimized to generate a sentence that closely aligns with \tilde{f} . To preserve the generative power of G , we keep it frozen and apply prefix-tuning [20], which prepends learnable tokens in the embedding space. We follow a test-time training approach to optimize learnable tokens for each test input on-the-fly. Our method builds upon the work of [3].

A high-level overview of this process is illustrated in Figure 2. Using a pre-trained language model G , we prepend randomly initialized learnable tokens, referred to as prefixes, which guide G to produce text that maximizes alignment with visual features. These learnable prefixes function as key-value pairs in each attention block, ensuring that every generated word can attend to them.

For each iteration j , at a timestep ts , we sample the top- Q tokens from the output distribution of G , denoted as G_{out} , which serve as possible continuations for the sentence. These Q candidate sentences are then encoded by a text encoder T , mapping them into the same embedding space as \tilde{f} . We compute the cosine similarity between each encoded sentence and \tilde{f} , resulting in Q similarity scores. These scores are normalized with softmax and define a target distribution used to train G_{out} via Cross-Entropy loss. The learnable prefixes are updated through backpropagation.

With the updated prefixes, G is run again, and the most probable token is selected as the next word. This process is repeated for a predefined number of timesteps (up to the desired sentence length) or until the $< . >$ token is generated. At the end of each iteration, a full sentence is generated. We conduct this process for 20 iterations, generating 20 sentences in total. The final output is chosen as the sentence with the highest similarity to the visual features \tilde{f} .

We also add the fluency loss from [3] as well as other token processing operations. We refer readers to [3] for more information. We use the small GPT-2 of 124M parameters as G . We also noticed that using a bigger G (e.g., GPT-2 medium) does not enhance performance, indicating that a decoder with basic language generation knowledge is sufficient.

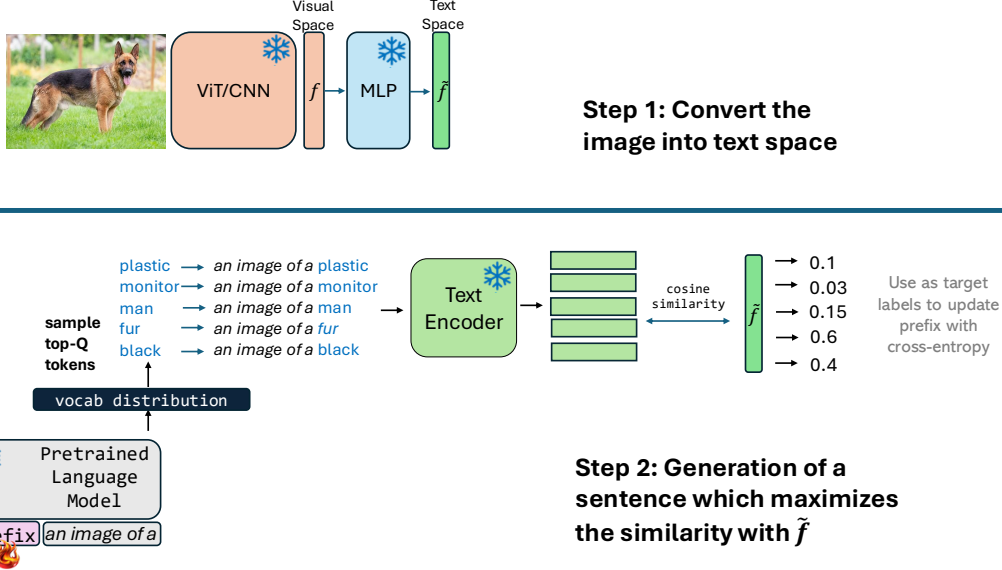


Figure 2: The process used to decode visual features of an image. The process is shown for the first timestep $ts = 1$ with a hard prompt set as “an image of a”.

I Using only class names

We remind readers from Section 3 that we only use the class names to formate the text prompt for the text encoder when training the MLP. In practice, we can go beyond class names by using resources like a class hierarchy from WordNet [66] (the original source where ImageNet was extracted from), or class descriptions extracted from a LLM as in CuPL [67] or VCVD[39]. However, this approach would be considered as “cheating. The original classifier implicitly learns the semantics, hierarchies, relationships and distinctive features of different classes. Explicitly providing additional information would not replicate the classifier faithfully since it would force the classifier to focus on predefined features or those we intend it to learn. Moreover, this would also leak information to downstream tasks such as CBMs and textual decoding of visual features, compromising the fairness of evaluation. For instance, if class descriptions were used in the training, the concepts in CBMs would align with those specified in the training prompts. For these reasons, we refrain from using any other additional information than the class names. We use the class names provided from <https://gist.github.com/yrevvar/942d3a0ac09ec9e5eb3a>.

J Compositional Captioning

The prompt we used for compositional captioning is as follows:

I will give you several attributes and verbs that are included in an image, each with a score. The score reflects how important (or how grounded) the attribute/verb is to the image, and higher means more important and grounded. Your job is to formulate a caption that describes the images by looking at the attributes/verbs with their associated scores. You should not reason or generate anything that is based on your own knowledge or guess. Everything you say has to be grounded in the attributes/verbs and score importances. Please use the following the structure, style, and pattern of the following examples. Example 1: A woman wearing a net on her head cutting a cake. Example 2: A child holding a flowered umbrella and petting a yak. Example 3: A young boy standing in front of a computer keyboard. Example 4: a boy wearing headphones using one computer in a long row of computers. Example 5: A kitchen with a stove, microwave and refrigerator. Example 6: A chef carrying a large pan inside of a kitchen.

Here are the attributes and scores: `{detected concepts with scores}`, and these are the verbs and scores: `{detected verbs with scores}`.

J.1 Domain-Specific Compositional Captioning

Next, we explore alternative concept sets in Compositional Captioning. In the main manuscript, we reported results using the 20,000 most common English words as our concept set. Since the LLM remains fixed and functions as a composer, integrating detected concepts and verbs grounded in the image into a caption, we can seamlessly substitute the concept set with any domain-specific concept set alternative. This allows for the generation of captions (here, decoded visual features) tailored to a specific domain. Here, we maintain the same set of verbs but explore the use of concepts specific to the ImageNet dataset. Since ImageNet lacks dedicated captions, we evaluate the domain-specific captioning by anticipating a decline in performance on the COCO captioning dataset. We use the ImageNet-specific concept set from [15] and report zero-shot captioning performance in Table 7. As shown, we observe a decrease in all metrics. This shows that our method can readily decode visual features into text for any domain. Finally, also note that we can control the style of the generations by simply prompting the LLM to compose the concepts and verbs in a specific style (e.g., humorous, positive, negative).

Method	B4	M	R-L	C	S
ZeroCap	2.6	11.5	—	14.6	5.5
ConZIC	1.3	11.5	—	12.8	5.2
Ours					
MobileNetv3-L	3.50	12.7	29.1	11.4	6.1
ResNet50	3.60	12.7	29.3	12.0	6.0
ResNet101v2	3.50	12.9	29.3	12.2	6.3
WideResNet101v2	3.70	12.9	29.6	12.4	6.2
ConvNeXt-Base	3.80	12.8	29.5	12.7	6.2
EfficientNetv2-S	3.70	12.9	29.6	12.9	6.3
ViT-B/16 (pt)	3.80	13.1	29.5	13.2	6.5
BeiT-L/16	3.90	13.2	29.6	13.4	6.6

Table 7: Composition Captioning Performance using the ImageNet-specific LF-CBM concept set

K Global Class-Wise Qualitative Examples

In Figure 3, we present a probability distribution of global class-wise concepts. These are concepts detected for all images of a specific class, along with their frequency. We consider two semantically similar classes but distinctively different: “hammerhead shark” and a “tiger shark”. We highlight in yellow the top concepts in “hammerhead shark” that are not present in “tiger shark”. These concepts are “harpoon” and “lobster hammer”, both which are distinctive to the head of the hammerhead shark and drive its prediction.

L Waterbirds/Landbirds Dataset

There are two challenges associated with using the Waterbirds-100 dataset [59] in our work. First, our method cannot transform a classifier trained on this dataset because learning meaningful text representations from merely two labels (waterbird and landbird) with our MLP is not feasible. Second, we cannot evaluate our ImageNet-trained models on this dataset due to its highly artificial nature, which results in numerous severe out-of-distribution samples for classifiers trained on ImageNet. Therefore, we manually curated our own waterbird/landbird dataset using ImageNet validation images. Specifically, for the waterbird images, we consider classes of birds from ImageNet that are at least 90% of the time found in water backgrounds—a statistic verified by manually inspecting 100 random training images of those birds. For those birds, we then select their images in the ImageNet validation set that appear on land backgrounds. We perform a similar procedure for the landbird class. For the landbird class, we encountered a problem. Although many ImageNet bird classes nearly always

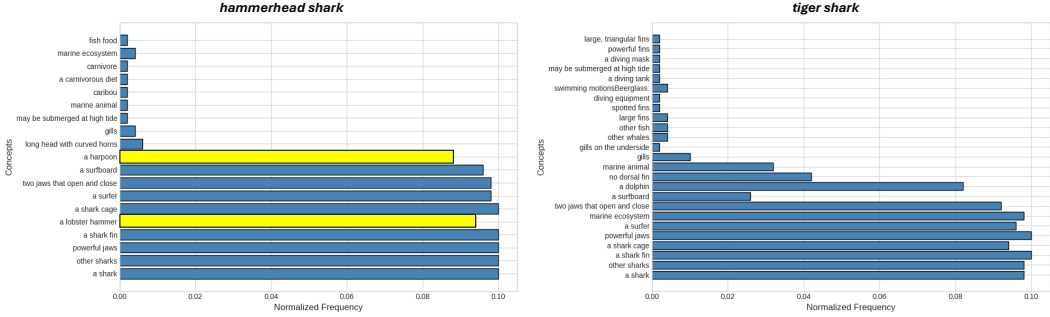


Figure 3: Global class-wise interpretability analysis with our Concept Bottleneck Model. We highlight in yellow the top concepts in "hammerhead shark" that are not present in "tiger shark", and therefore distinctive to "hammerhead shark".

feature land backgrounds in their training images, we were unable to find a substantial number of validation images depicting these birds against water backgrounds (e.g., we could not find any image of the bird *robin* with water background in the ImageNet validation set). In order to solve this issue, we utilized the Stable Diffusion 2.1 [68] text-to-image generative model to generate images of those birds on water backgrounds. We ensured that the generated images of those birds have the correct physical and distinctive features of the bird. For all images, we always ensure that the background (water/land) is clearly visible. This leads us to a validation dataset of 140 images (70 images for each class). Specifically, for the waterbird class, all 70 images coming from the ImageNet validation set. For the landbirds class, 15 images come from the ImageNet validation set, and 55 are generated with Stable Diffusion.

M Multi-class CBM Intervention Classes and Concepts

Class	Concepts
tench	fish, freshwater, fins, dorsal, olive
english springer	dog, long ears, brown and white, playful, hunting
cassette player	portable, audio, tape, speakers, buttons
chainsaw	sharp, handheld, cutting, metal, wood
church	cross, tower, architecture, sacred, religious
french horn	curved, mouthpiece, musical instrument, orchestral, blow
garbage truck	large vehicle, wheels, clean, high load, lift
gas pump	fueling, hose, metallic, gasoline, handle
golf ball	small, white, round, rubber, dimples
parachute	fabric, fly, air, landing, strings

Table 8: ImageNet classes and their five associated concepts we use in our multi-class CBM intervention experiment.